Available online at www.sciencedirect.com
ScienceDirect
Journal of the European Ceramic Society 28 (2008) 2573–2580
www.elsevier.com/locate/jeurceramsoc

Role of urea addition in the preparation of tetragonal $BaTiO_3$ nanoparticles using flame-assisted spray pyrolysis

Yoshitake Terashi [a], Agus Purwanto [b], Wei-Ning Wang [b], Ferry Iskandar [b], Kikuo Okuyama [b,*]

[a] *R&D Center-Kyocera Corporation, 1-4 Yamashita-Cho, Kokubu, Kagoshima 899-4312, Japan*
[b] *Department of Chemical Engineering, Graduate School of Engineering, Hiroshima University, 1-4-1 Kagamiyama, Higashi Hiroshima, Hiroshima 739-8527, Japan*

Received 29 November 2007; received in revised form 27 February 2008; accepted 6 March 2008

Abstract

In this study, flame-assisted spray pyrolysis (FASP) was used to produce $BaTiO_3$ nanoparticles with relatively high tetragonality and controlled sizes from 23 to 33 nm in a one-step process. The addition of urea into the precursor is the key factor for the formation of tetragonal $BaTiO_3$ nanoparticles; the lack of urea addition led to the formation of submicrometer $BaTiO_3$. The formation of $BaTiO_3$ nanoparticles was suggested from the disintegration of submicrometer particles due to the decomposition of urea presented in the interconnection of their primary particles. Also, combustion of the decomposed gases of urea produced additional heat, which improved the tetragonality of the $BaTiO_3$ nanoparticles. Tetragonality was enhanced from 1.0051 to 1.0071 by increasing the urea addition to as high as 4 M. The results of the present study show that addition of urea to the precursor is an effective strategy for the direct production of tetragonal $BaTiO_3$ nanoparticles using the FASP method.

Keywords: $BaTiO_3$; Tetragonality; Flame; Aerosol; Continuous process

1. Introduction

$BaTiO_3$ powder has been used extensively in the electronics industry for fabrication of multi-layer ceramic capacitors (MLCCs). Miniaturization of electronic devices requires smaller components, including capacitors of reduced size.[1,2] To make smaller ceramic capacitors, the $BaTiO_3$ particles also must be very small ($\leq$200 nm) and must exhibit high permittivity. However, the permittivity decreased when the size of $BaTiO_3$ particles was reduced to below 1 μm.[3]

Generally, the permittivity of $BaTiO_3$ particles depends on particle size,[3,4] tetragonality,[5] the Ba/Ti ratio,[6] and the material used to coat the $BaTiO_3$ particles.[1,7] The increasing tetragonality of $BaTiO_3$ particles leads to the enhancement of their permittivity. This enhancement is a result of the asymmetry of the crystal structure that displaces titanium ions from the centrosymmetric position within the TiO_6 octahedron.[8] In addition, the tetragonality of $BaTiO_3$ is influenced by its particle size. Above a critical size, increasing of particle size of $BaTiO_3$ leads to an enhancement of tetragonality.[9–11] The critical size is where the crystal structure of $BaTiO_3$ shifts from the cubic to the tetragonal phase—approximately 16 nm (based on empirical estimation).[12] Experimentation has shown that the critical size ranges from 25[10] to 190 nm[11], depending on the preparation method.

$BaTiO_3$ particles can be prepared using various processes: hydrothermal,[5,8] glycothermal,[13] precipitation,[14] spray pyrolysis (SP),[15–17] low pressure spray pyrolysis (LPSP),[18] radio-frequency plasma chemical vapor deposition (RF-CVD),[19] and flame-assisted spray pyrolysis (FASP).[2,20] Among these processes, FASP has the advantage of producing dry materials with less impurities and high crystallinity in fast and continuous mode. The preparation of large $BaTiO_3$ particles (microns in size) by this method has been reported.[20] And, due to their large sizes, the prepared particles have good tetragonality. Recently, we reported the preparation of $BaTiO_3$ nanoparticles using flame-assisted spray pyrolysis (FASP).[2] The average size of the prepared particles ranged from 23 to 71 nm. However, the crystal structure of the $BaTiO_3$ nanoparticles was cubic.

There have been many attempts to prepare $BaTiO_3$ nanoparticles in a tetragonal phase. The general method is by the annealing

* Corresponding author. Tel.: +81 82 424 7716; fax: +81 82 424 5494.
E-mail address: okuyama@hiroshima-u.ac.jp (K. Okuyama).

0955-2219/$ – see front matter © 2008 Elsevier Ltd. All rights reserved.
doi:10.1016/j.jeurceramsoc.2008.03.002

of amorphous or cubic $BaTiO_3$ nanoparticles at an elevated temperature for extended periods of time. This technique has been used to produce tetragonal $BaTiO_3$ particles in processes such as hydrothermal,[21] sol–crystal,[22] RF-CVD,[19] etc. In the case of RF-CVD, the as-prepared $BaTiO_3$ particles (cubic, 21.6 nm) were transformed to tetragonal $BaTiO_3$ nanoparticles (tetragonality 1.0007, 32 nm) after being annealed at temperatures as low as 550 °C for 1 h. Another technique is by the application of an additive to the precursor prior to processing. This technique was shown in the preparation of tetragonal $BaTiO_3$ by salt-assisted-SP (SASP)[17] and citric acid-assisted-SP (CASP).[16] In SASP, washing of the as-prepared particles is required for removal of the salt and the disintegration of large particles into nanoparticles. The as-prepared particles from CASP were milled to produce tetragonal $BaTiO_3$ nanoparticles.[16] In both techniques, the required additional treatments led to an increase of energy usage and time consumption.

In this paper, a new technique for the production of tetragonal $BaTiO_3$ nanoparticles using urea as a precursor additive in the FASP method is described. The addition of urea into precursor facilitates the formation of tetragonal $BaTiO_3$ nanoparticles in a single-step process. Urea was introduced to manipulate the crystallinity and morphology of the as-prepared $BaTiO_3$ particles. The addition of urea, which fully decomposed at temperature of 360 °C, is useful for the disintegration of primary particles producing $BaTiO_3$ nanoparticles. Furthermore, the heat evolved from combustion of the decomposed gases with oxygen, resulted in local heating of the nanoparticles. Consequently, the additional heat resulting from urea combustion improved the tetragonality of the $BaTiO_3$ nanoparticles.

2. Experimental

The experimental setup of flame-assisted spray pyrolysis (FASP) is shown elsewhere.[2] The system consists of an aerosol generator, a diffusion flame reactor and a powder collection system. An ultrasonic nebulizer was used to generate droplets of precursor at a frequency of 1.7 MHz. The atomized droplets were transported to the flame by a carrier gas. The flame was maintained by flowing methane and oxygen gases, which served as the fuel and the oxidant, respectively. The ratio of oxidant to fuel was 2.5. The prepared particles were collected in the powder collector.

The precursor chemicals used in this experiment were $(CH_3COO)_2Ba$ (barium acetate, 99%), aqueous $TiCl_4$ solution (titanium chloride, TCl-36, 36%) and NH_2CONH_2 (urea, 99%). $(CH_3COO)_2Ba$ and NH_2CONH_2 were purchased from Kanto Chemical Co. Inc. (Tokyo, Japan) and were used without purification. Aqueous $TiCl_4$ solution was obtained from Showa Co. Inc., Japan. Commercial $BaTiO_3$ nanoparticles, 30 nm in size (lot. number: 040201, Toda Kogyo Inc., Hiroshima, Japan), were used for comparison. To evaluate the dependence of tetragonality on particle size, the total precursor concentration was varied from 0.05 to 0.2 M. In all experiments, precursors were prepared using a Ba:Ti molar ratio of 1:1. Urea was added to the precursor at a maximum concentration of 4 M. To prepare homogeneous solutions, all chemicals were dissolved in water and then mixed using a magnetic stirrer for several hours. After mixing, the precursor solution was added to the nebulizer tank for atomizing.

To evaluate the thermal properties of the precursor under heat treatment, thermal gravimetric (TG) and differential thermal analysis (DTA) (TG–DTA 6200, Seiko Instruments Inc., Tokyo, Japan) were used. The TG–DTA analysis was carried out by placing a sample of approximately 10 mg in a platinum pan. The temperature was then increased from 30 to 1000 °C at a heating rate of 10 °C/min under flowing air (200 mL/min).

Droplet size was measured using a spray particle analyzer system (Spraytec, Malvern Instruments Ltd., Malvern, U.K.), which is a diode laser-based system with a wavelength of 670 nm and a beam diameter of 10 mm. The droplets were measured continuously with measurement rates as high as 2.5 kHz. The measurement was done using a 100-mm lens, the measurable droplet size ranged from 0.1 to 230 μm.

Particles were characterized using field-emission scanning electron microscopy (FE-SEM), transmission electron microscopy (TEM), and X-ray diffractometry (XRD). FE-SEM (Hitachi S-5000) was used to observe particle morphology. The geometric mean diameter (GMD, d_g) and geometric standard deviation (GSD, σ_g) were calculated using the equations $\log d_g = \left(\sum n \log d\right) / \left(\sum n\right)$, and $\log \sigma_g = \left\{\sum \left[n(\log d - \log d_g)^2 / \sum n\right]\right\}^{1/2}$, respectively, from the corresponding FE-SEM images by randomly sampling about 200 particles, using d as the particle size. The morphology and electron diffraction of the crystals were examined in detail using TEM (JEM-3000F, JEOL Ltd., Tokyo, Japan) at 300 kV. Particle crystallinity was determined using selected area electron diffraction (SAED) coupled with TEM. The crystallite phase and purity of the prepared particles were also examined by XRD (RINT 2200V, Rigaku-Denki Corp., Tokyo, Japan).

3. Results and discussion

3.1. Thermal analysis of precursors

To clearly understand the urea effect addition to the precursor during the heating process, TG–DTA analysis of the precur-

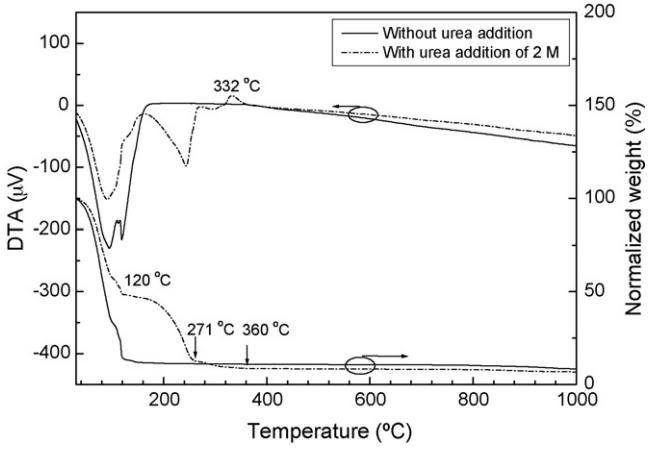

Fig. 1. Thermal gravimetric–differential thermal analysis (TG–DTA) graph of the precursor with and without urea addition.

sor with and without addition of urea was first carried out as shown in Fig. 1. The precursor without urea started to decompose at 120 °C. With urea, the TG profile indicated additional decomposition of the urea at temperatures ranging from 120 to 360 °C. In the literature, it is reported that urea decomposes into biuret at temperatures ranging from room temperature to 190 °C. At higher temperatures, biuret decomposes into cyanuric acid, ammelide and melamine. Urea completely decomposes at 360 °C.[23] The overall decomposition reaction of urea under heat treatment in the presence of water can be written as[24]

$$NH_2CONH_2 + H_2O \rightarrow 2NH_3 + CO_2$$

Based on the above reaction equation, 1 mol of urea produces 3 mol of decomposed gases. The TG–DTA results show that addition of urea contributes additional heat and gas evolution that are expected to have an effect on the crystallinity improvement and particle disintegration during the flame process. The detailed investigation will be shown in the following sections.

3.2. Morphology and size control of $BaTiO_3$ nanoparticles

To evaluate the role of urea addition on the morphology of the prepared $BaTiO_3$ particles, different concentrations of urea (0–4 M) corresponding to urea-precursor molar ratios ranging from 0 to 20, were added to the precursor. The $BaTiO_3$ powder

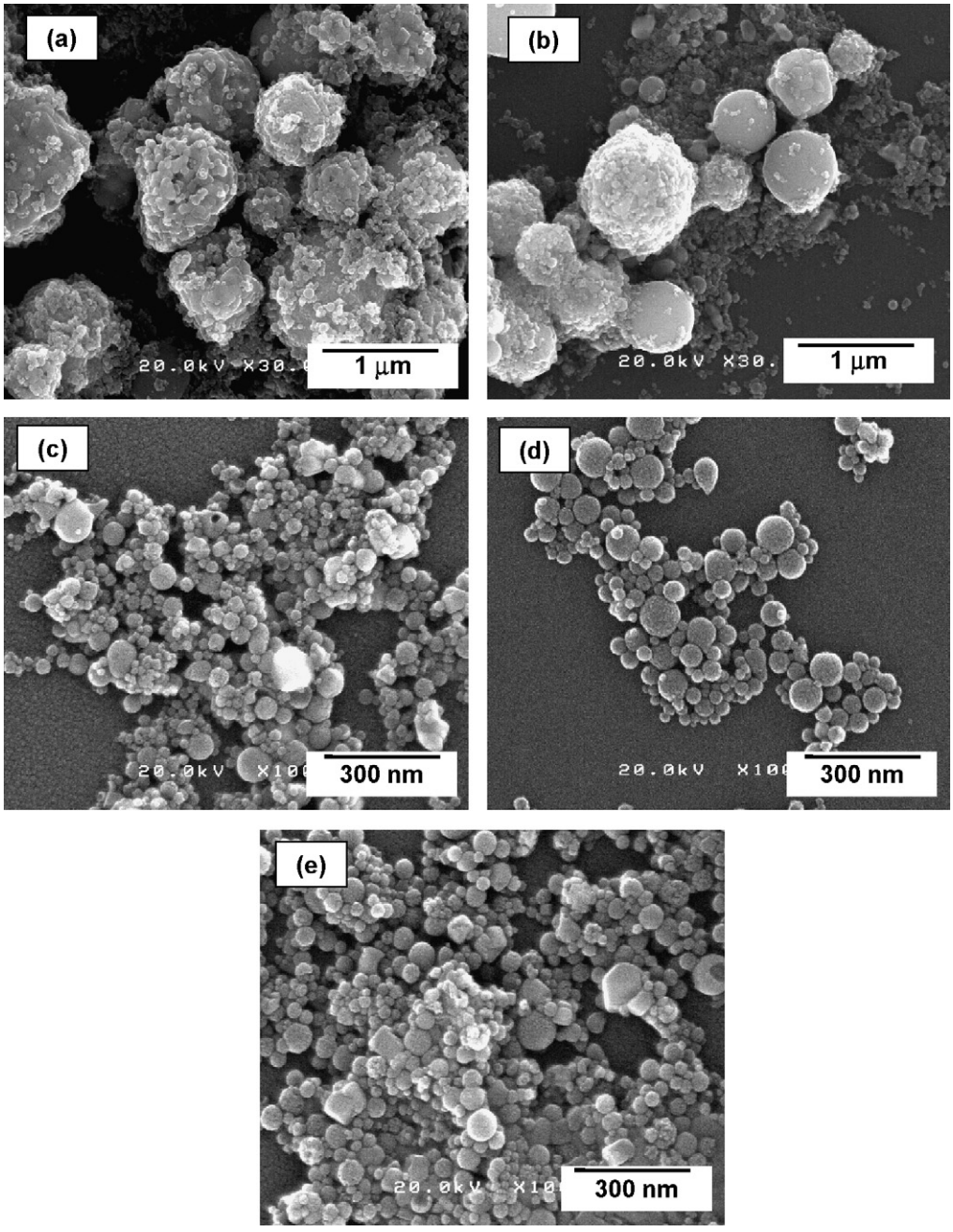

Fig. 2. Field emission scanning microscopy (FE-SEM) images of $BaTiO_3$ particles prepared from precursor without urea addition (a), with urea addition of 1 M (b), 2 M (c), 3 M (d) and 4 M (e).

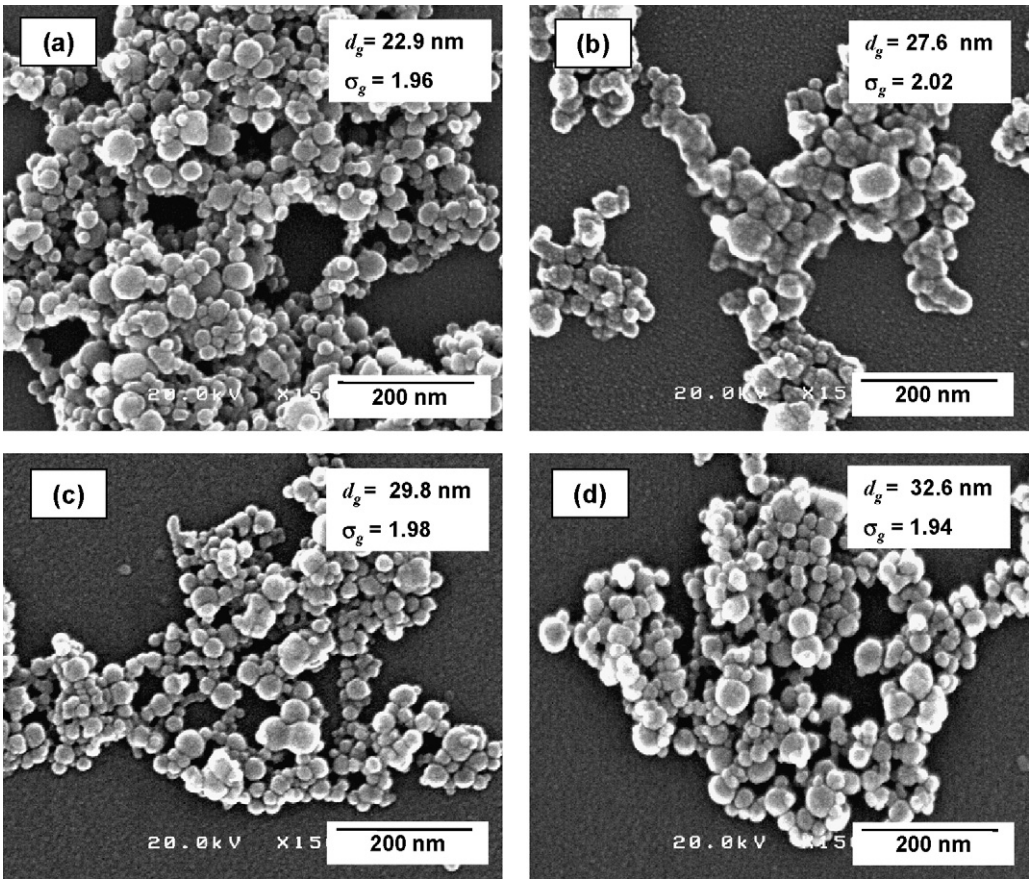

Fig. 3. Field emission-scanning electron microscopy (FE-SEM) images of $BaTiO_3$ particles prepared from precursor concentration of 0.05 M (a), 0.075 M (b), 0.1 M (c) and 0.2 M (d).

was prepared using a CH_4 flow rate of 3 L/min with an O_2 carrier gas flow rate of 10 L/min.

Fig. 2 shows FE-SEM images of the $BaTiO_3$ particles prepared from the precursor with and without the addition of urea. Without added urea, the as-prepared $BaTiO_3$ particles were primarily sub-micron in size (300–800 nm); a small fraction of the particles were nano-sized, as shown in Fig. 2a. Addition of urea to the precursor significantly affected the morphology of the prepared particles. When 1 M of urea was added to the precursor, the quantity of nanoparticles increased while the size of larger particles reduced, as shown in Fig. 2b. In the case of urea addition of 2 M or more, dispersed nano-sized $BaTiO_3$ particles were obtained as indicated in Fig. 2c–e.

In addition, concentration of precursor is one of the parameters that can be used to control particle size in aerosol processes.[2] In the present study, $BaTiO_3$ particles of different sizes were produced by varying the precursor concentrations from 0.05 to 0.2 M. Precursors were prepared with a molar ratio of urea to precursor of 20. Fig. 3 shows the FE-SEM images of the particles prepared using different concentrations. The produced particles had geometric mean sizes of 22.9, 27.6, 29.8 and 32.6 nm for precursor concentrations of 0.05, 0.075, 0.1 and 0.2 M, respectively. The geometric standard deviations of the corresponding particles were approximately 2, indicating a rather broad particle size distribution.

3.3. Crystalinity and tetragonality of $BaTiO_3$ nanoparticles

XRD patterns of the $BaTiO_3$ nanoparticles prepared with different concentrations of urea additive (varied from 0 to 4 M) are shown in Fig. 4a. The $BaTiO_3$ nanoparticles were prepared from a precursor concentration of 0.2 M. The prepared $BaTiO_3$ particles had tetragonal structures (space group: *p4mm*), which is consistent with JCPDS Reference No. 05-0626. The crystallite sizes were 18.3, 22.5, 24.8 and 25.3 nm for the particles prepared without and with urea addition of 1, 2 and 4 M, respectively. Adding high concentrations of urea to the precursor caused $BaTiO_3$ nanoparticles with high crystallinity to form. This was confirmed by the magnified XRD patterns for high urea contents ranging from 44° to 46° as shown in Fig. 4a (right hand side). In addition, the tetragonality (ratio of c to a) of the $BaTiO_3$ nanoparticles increased from 1.00509 to 1.00710 with high urea concentrations, as shown in Fig. 4b.

The improvement of crystallinity and tetragonality of $BaTiO_3$ nanoparticles, as an effect of urea addition, can be explained as follows. As shown in Fig. 1 of the TG–DTA analysis, it was found that the decomposition of urea releases additional heat. The exothermic peak is shown at 332 °C. After adding 4 M urea to a 0.2 M precursor solution, every droplet released approximately 1.48×10^{-5} J of energy, as calculated based on the combustion enthalpy of urea. Based on stoichiometric cal-

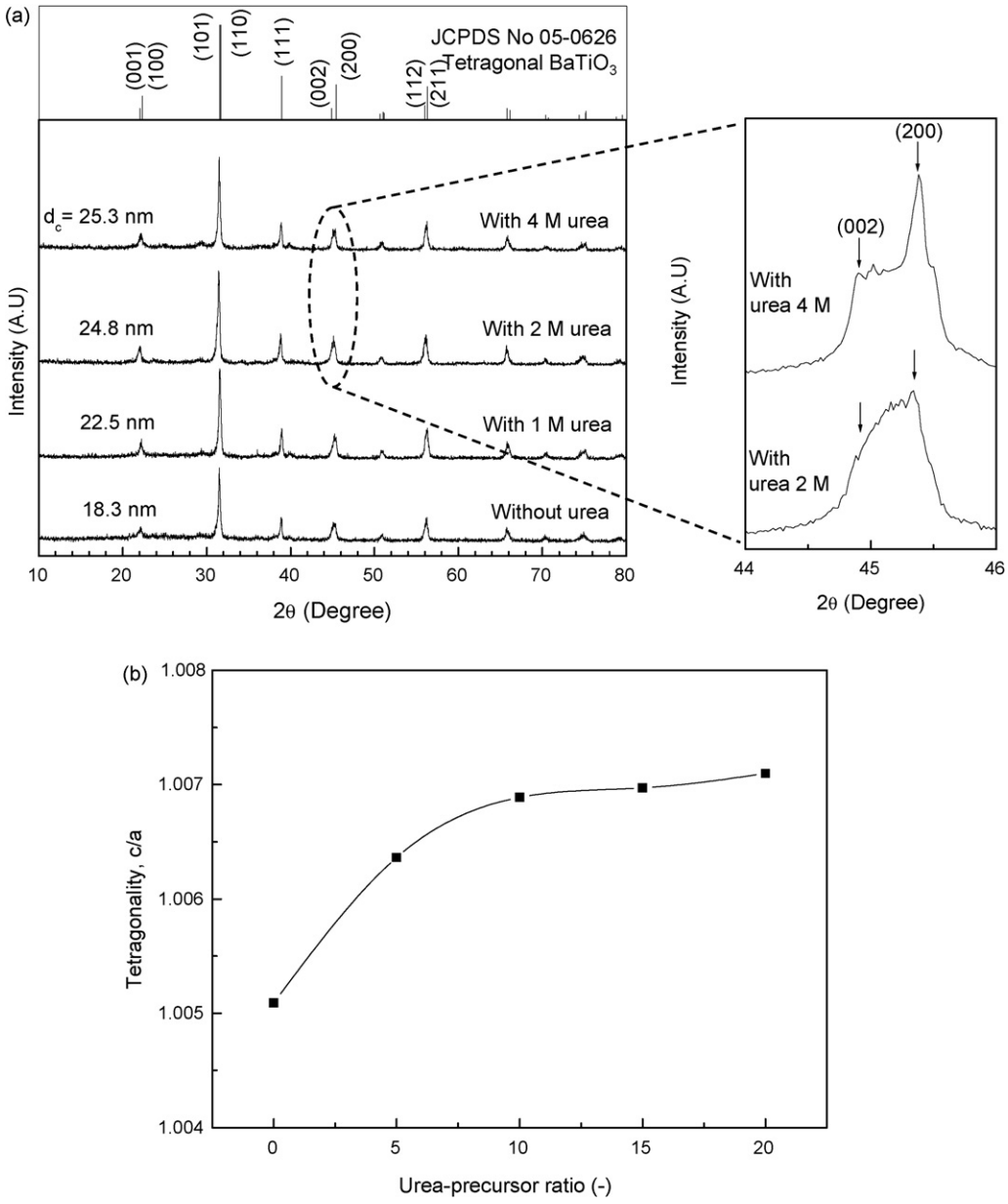

Fig. 4. X-ray diffraction (XRD) pattern of $BaTiO_3$ powder prepared from precursor without and with urea addition (left hand side), and magnified XRD patterns for high urea contents ranging from 44° to 46° (right hand side) (a) and tetragonality of the corresponding particles (b).

culations, every droplet of precursor produced 9.7×10^{-15} mol $BaTiO_3$ particles. From the comparison of heat released from urea and mol number of the produced $BaTiO_3$, it is known that the heat released from urea combustion is high enough to contribute to $BaTiO_3$ crystal growth. Thus, the production of $BaTiO_3$ nanoparticles with high tetragonality is easily understood from the additional heat of urea combustion.

The tetragonality of the $BaTiO_3$ nanoparticles prepared from the different precursor concentrations was evaluated using XRD analysis as shown in Fig. 5. In this XRD pattern, the tetragonal structure of $BaTiO_3$ is indicated by the splitting of the (2 0 0) and (0 0 2) planes at 2θ from 44° to 46°. Tetragonality was calculated as the relative ratio of the lattice parameter *c*- to *a*-axes. The tetragonality values of $BaTiO_3$ nanoparticles were 1.00566, 1.00576, 1.00648 and 1.00710 for particles prepared using concentrations of 0.05, 0.075, 0.1 and 0.2 M, respectively. It is shown that the result is in agreement with the previous finding in which the tetragonality of $BaTiO_3$ nanoparticles increased as the particle size increased.[10,25]

3.4. Suggested mechanism of nanoparticle formation with urea addition

As described above, the addition of urea to the precursor significantly affected particle morphology and size. In FASP, the liquid precursor was atomized into droplets prior to transport to the flame zone. The atomized droplets will undergo solvent evaporation, solute precipitation, nucleation, intraparticle reaction, coagulation, sintering and densification to form the final

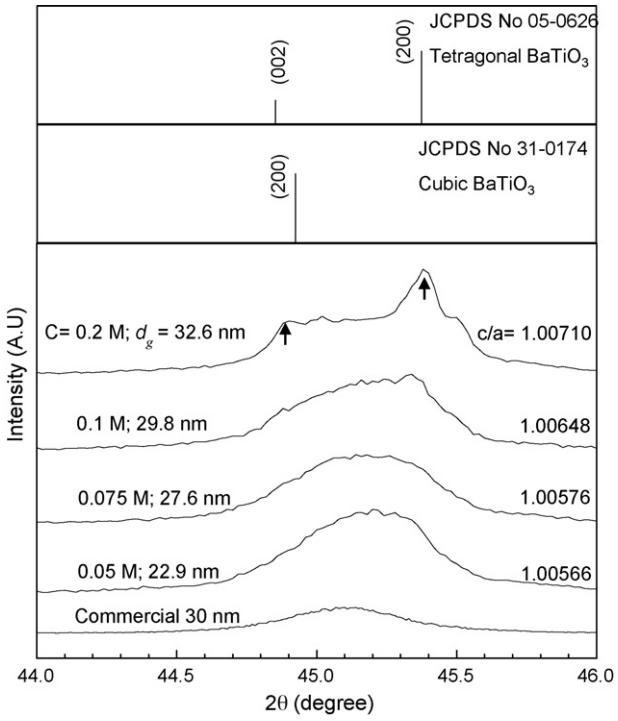

Fig. 5. X-ray diffraction (XRD) pattern of $BaTiO_3$ powder prepared using different concentrations of precursor.

particles.[2] The droplet size has strong relativity to precursor properties and subsequently the final product particle size.[26] To investigate the effect of urea addition into the precursor, droplet size was evaluated using a droplet size analyzer. The measured droplet size was approximately 5.7 μm and was not significantly altered with variation of the urea concentrations. The sub-micron order of $BaTiO_3$ particles should be prepared from the calculation of the one-droplet-to-one-particle (ODOP) principle. In fact, Fig. 2 shows that as-prepared particles in the nano-sized order indicate they were produced from a one-droplet-to-many-particles (ODMP) mechanism.

Fig. 6 shows the schematic diagram explaining the formation of nanoparticles as an effect of urea addition into the precursor. Early in the flame process, evaporation of droplets produced dried particles which contained dried urea and the precipitated precursor. The presence of urea in the dried particles prevented the interconnection between precipitated particles. With further heating by flame, urea decomposed and primary particles disintegrated producing nanoparticles. This mechanism is almost similar to that of the salt-assisted spray pyrolysis process in which dried salt prevents an interconnection between precipitated particles.[17] The advantage of the urea addition in FASP is that washing of the additive is unnecessary because urea can be decomposed directly in the flame.

Disintegration of sub-micron particles into nanoparticles by evolution of gases from organic material decomposition also occurs in batch processes. The phosphor materials, $SrTiO_3$:Pr,Al and $(Y,Gd)_3Al_5O_{12}$:Ce, were investigated as models.[27] Particles prepared using spray pyrolysis with the polymer were annealed at high temperatures. Gas evolution during the heating process can be used to cause disintegration of sub-micron particles into nanoparticles. In low pressure spray pyrolysis (LPSP), the addition of urea, in conjunction with the low pressure within the reactor, was shown to be a primary determinant of $BaTiO_3$ nanoparticle formation.[18]

3.5. Comparison with commercial $BaTiO_3$ particles

Then, to evaluate the characteristics of the as-prepared $BaTiO_3$ nanoparticles by FASP, a comparison with commercial particles was conducted. The TEM images of as-prepared and commercial $BaTiO_3$ nanoparticles are shown in Fig. 7. Commercial $BaTiO_3$ nanoparticles (supplied by Toda Kogyo Inc., Japan) were approximately 30 nm in size and formed agglomerates (Fig. 7a and b). In contrast, urea-assisted FASP produced non-agglomerated $BaTiO_3$ particles that were well-dispersed (Fig. 7c–f). Commercial particles were made using a wet synthesis method, which included an annealing step. Annealing processes tend to produce agglomerated particles. In the case of flame-assisted processes, $BaTiO_3$ particles were produced after a very short residence time. Rapid heating of particles prevented the formation of agglomerated particles. Furthermore, addition of urea to the precursor, as explained above, also contributed to the formation of dispersed $BaTiO_3$ nanoparticles. The TEM images show that $BaTiO_3$ particles produced using a flame-assisted process have a broad size distribution. In addition, the HRTEM images and diffraction pattern indicated that commercial $BaTiO_3$ is polycrystalline, whereas FASP-produced $BaTiO_3$ is single crystalline.

From the results, it was shown that $BaTiO_3$ nanoparticles with a tetragonal structure could be prepared directly from their aqueous precursor with the addition of urea by the FASP method. To be industrially applicable, the preparation process of nanoparticles could easily be scaled up for high production rate. FASP is one of the processes that have been scaled-up for silica and titania nanoparticles production. Thus, using the proposed method,

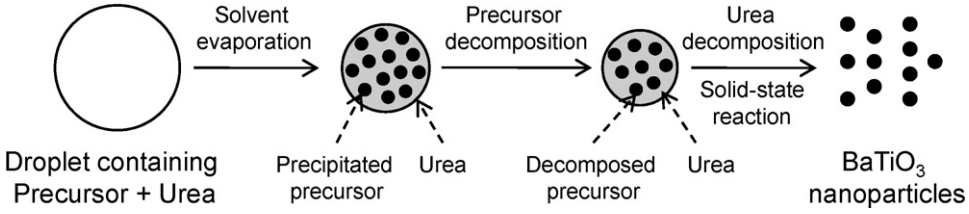

Fig. 6. Schematic diagram of the nanoparticle-formation mechanism using urea as a precursor additive.

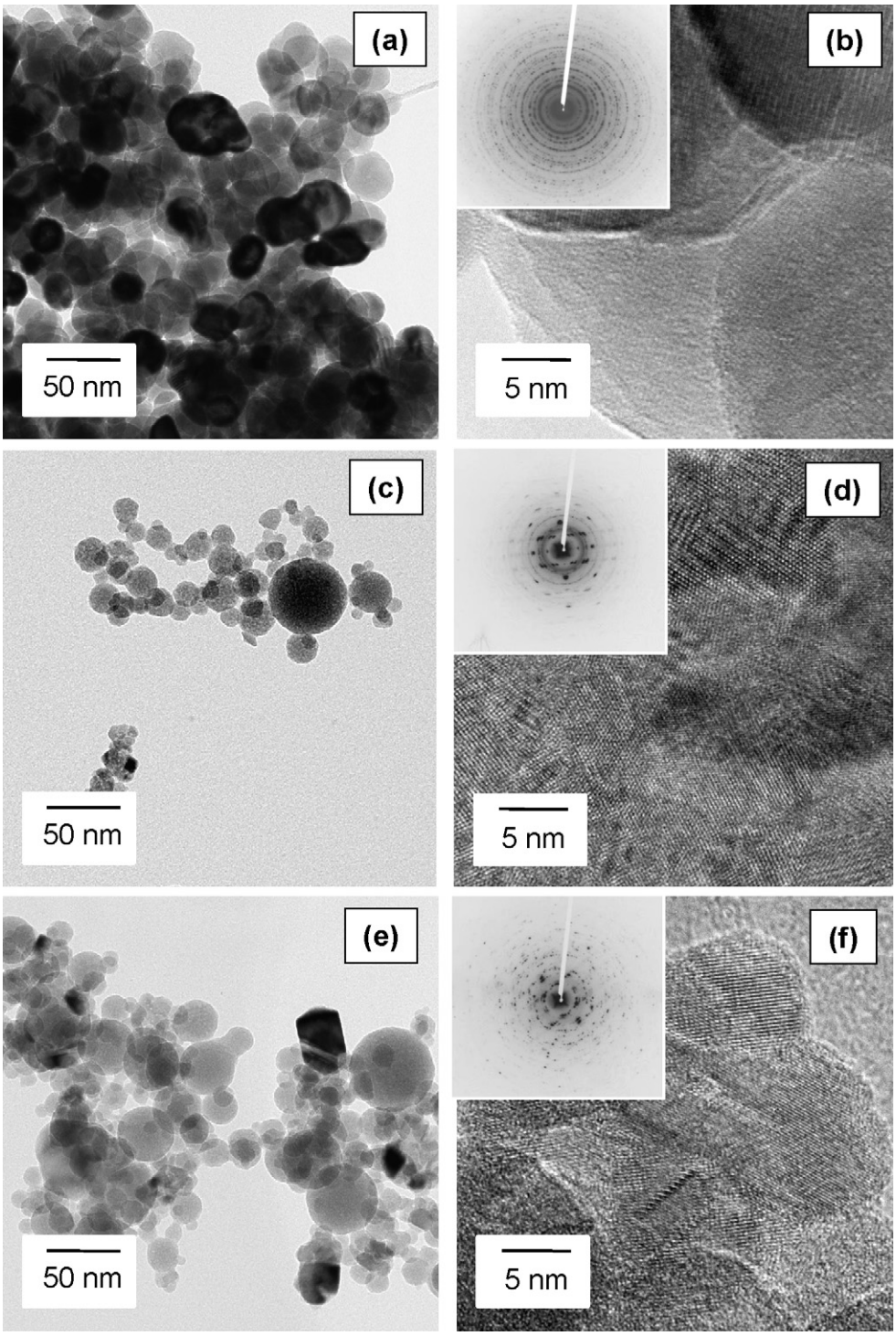

Fig. 7. Transmission electron microscopy (TEM) images of commercial $BaTiO_3$ nanoparticles (a and b) prepared from precursor with concentrations of 0.075 M (c and d) and 0.2 M (e and f).

production of tetragonal $BaTiO_3$ nanoparticles is possible on an industrial scale.

4. Conclusion

Tetragonal $BaTiO_3$ nanoparticles were synthesized using FASP from an aqueous precursor with urea addition in a single-step process. Addition of urea to the precursor affected both particle morphology and crystallinity. The addition of urea, which decomposed into gases during the flame process, caused disintegration of the interconnected primary particles. This process led to the formation of $BaTiO_3$ nanoparticles. Additional heat produced by combustion of the decomposed gases contributed to improved crystallinity, as indicated by the high tetragonality of the prepared $BaTiO_3$ nanoparticles. Nanoparticle size and tetragonality could also be controlled by varying

the precursor concentration. Compared with the commercial $BaTiO_3$ nanoparticles, the as-prepared particles showed less agglomeration. Thus, the results of the present study show that addition of urea to the precursor is an effective method for the production of $BaTiO_3$ nanoparticles with relatively high tetragonality using FASP.

Acknowledgements

The authors thank the Ministry of Education, Culture, Sports, Science and Technology of Japan for providing a doctoral scholarship (A.P), a JSPS (Japan Society for the Promotion of Science) post-doctoral fellowship (W.N.W) and a grant-in-aids for scientific research (K.O).

References

1. Buscaglia, M. T., Viviani, M., Zhao, Z., Buscaglia, V. and Nanni, P., Synthesis of $BaTiO_3$ core–shell particles and fabrication of dielectric ceramics with local graded structure. *Chem. Mater.*, 2006, **18**, 4002–4010.
2. Purwanto, A., Wang, W. N., Lenggoro, I. W. and Okuyama, K., Formation of $BaTiO_3$ nanoparticles from an aqueous precursor by flame assisted spray pyrolysis. *J. Eur. Ceram. Soc.*, 2007, **27**, 4489–4497.
3. Arlt, G., Hennings, D. and With, G. D., Dielectric properties of fine-grained barium titanate ceramics. *J. Appl. Phys.*, 1985, **58**, 1619–1625.
4. Buscaglia, V., Buscaglia, M. T., Viviani, M., Mitoseriu, L., Nani, P., Trefiletti, V., Piaggio, P., Gregora, I., Ostapchuk, T., Pokorny, J. and Petzelt, J., Grain size and grain boundary-related effect on the properties of nanocrystalline barium titanate ceramics. *J. Eur. Ceram. Soc.*, 2006, **26**, 2889–2898.
5. Xu, H. and Gao, L., Tetragonal nanocrystalline barium titanate powder: preparation, characterization and dielectric properties. *J. Am. Ceram. Soc.*, 2003, **86**, 203–205.
6. Pinceloup, P., Courtois, C., Leriche, A. and Thierry, B., Hydrothermal synthesis of nanometer-sized barium titanate powder: control of barium/titanate ratio sintering and dielectric properties. *J. Am. Ceram. Soc.*, 1999, **82**, 3049–3056.
7. Park, M. B., Cho, N. H., Kim, C. D. and Lee, S. K., Phase transition and physical characteristics of nanograined $BaTiO_3$ ceramics synthesized form surface-coated nanopowders. *J. Am. Ceram. Soc.*, 2004, **87**, 510–512.
8. Clark, I. J., Takeuchi, T., Ohtori, N. and Sinclair, D. C., Hydrothermal synthesis and characterization of $BaTiO_3$ fine powders: precursors, polymorphism, and properties. *J. Mater. Chem.*, 1999, **9**, 83–91.
9. Buscaglia, M. T., Viviani, M., Buscaglia, V., Mitoseriu, L., Testino, A., Nanni, P., Zhao, Z., Nygren, M., Harnagea, C., Piazza, D. and Galassi, D., High dielectric constant and frozen macroscopic polarization in dense nanocrystalline $BaTiO_3$ ceramics. *Phys. Rev. B: Condens. Matter*, 2006, **73**, 064114-1–064114-10.
10. Hoshina, T., Kakemoto, H., Tsurumi, T., Wada, S. and Yashima, M., Size and temperature induced phase transition behaviors of barium titanate nanoparticles. *J. Appl. Phys.*, 2006, **99**, 054311-1–054311-8.
11. Begg, B. D., Vance, E. R. and Nowotny, J., Effect of particle size on the room-temperature crystal structure of barium titanate. *J. Am. Ceram. Soc.*, 1994, **77**, 3186–3192.
12. Aoyagi, S., Kuroiwa, Y., Sawada, A., Kawaji, H. and Atake, T., Size effect on crystal structure and chemical bonding nature in $BaTiO_3$ nanopowder. *J. Therm. Anal. Calorim.*, 2005, **81**, 627–630.
13. Jung, Y. J., Lim, D. Y., Nho, J. S., Cho, S. B., Riman, R. E. and Lee, B. W., Glycothermal synthesis and characterization of tetragonal barium titanate. *J. Cryst. Growth*, 2005, **274**, 638–652.
14. Yoon, S., Baik, S., Kim, M. G., Shin, N. and Kim, I., Synthesis of tetragonal barium titanate nanoparticles via alkoxide–hydroxide sol-precipitation: effect of water addition. *J. Am. Ceram. Soc.*, 2007, **90**, 311–314.
15. Lee, S., Son, T., Yun, J., Kwon, H., Messing, G. L. and Jun, B., Preparation of $BaTiO_3$ nanoparticles by combustion spray pyrolysis. *Mater. Lett.*, 2004, **58**, 2932–2936.
16. Lee, K. K., Kang, Y. C., Jung, K. Y. and Kim, J. H., Preparation of nano-sized $BaTiO_3$ particles by citric acid-assisted spray pyrolysis. *J. Alloys Compd.*, 2005, **395**, 280–285.
17. Itoh, Y., Lenggoro, I. W., Madler, L. and Pratsinis, S. E., Size tunable synthesis of highly crystalline $BaTiO_3$ nanoparticles using salt assisted spray pyrolysis. *J. Nanopart. Res.*, 2003, **5**, 191–198.
18. Wang, W. N., Lenggoro, I. W., Terashi, Y., Wang, Y. C. and Okuyama, K., Direct synthesis of barium titanate nanoparticles via a low pressure spray pyrolysis method. *J. Mater. Res.*, 2005, **20**, 2873–2882.
19. Suzuki, K. and Kijima, K., Phase transformation of $BaTiO_3$ nanoparticles synthesized by RF-plasma CVD. *J. Alloys Compd.*, 2006, **419**, 234–242.
20. Brewster, J. H. and Kodas, T. T., Generation of unagglomerated, dense $BaTiO_3$ particles by flame-spray pyrolysis. *AIChE J.*, 1997, **43**, 2665–2669.
21. Lee, J. H., Nersisyan, H. H., Lee, H. H. and Won, C. W., Structural change of hydrothermal $BaTiO_3$ powder. *J. Mater. Sci.*, 2004, **39**, 1397–1401.
22. Takeuchi, T., Tabuchi, M., Ado, K., Hojo, K., Nakamura, O., Kageyama, H., Suyama, Y., Ohtori, N. and Nagasawa, M., Grain size dependence of dielectric properties of ultrafine $BaTiO_3$ prepared by a sol–crystal method. *J. Mater. Sci.*, 1997, **32**, 4053–4060.
23. Schaber, P. A., Colson, J., Higgins, S., Thielen, D., Anspach, B. and Brauer, J., Thermal decomposition (pyrolysis) of urea in an open reaction vessel. *Thermochim. Acta*, 2004, **424**, 131–142.
24. Fang, H. L. and DaCosta, H. F. M., Urea thermolysis and NOX reduction with and without SCR catalysts. *Appl. Catal., B*, 2003, **46**, 17–34.
25. Yashima, M., Hoshina, T., Ishimura, D., Kobayashi, S., Nakamura, W., Tsurumi, T. and Wada, S., Size effect on the crystal structure of barium titanate nanoparticles. *J. Appl. Phys.*, 2005, **98**, 014313-1–014313-8.
26. Wang, W. N., Purwanto, A., Lenggoro, I. W., Okuyama, K., Chang, H. K. and Jang, H. D., Investigation on the correlation between droplet and particle size distribution in ultrasonic spray pyrolysis. *Ind. Eng. Chem. Res.*, 2008, **47**, 1650–1659.
27. Wang, W. N., Kim, S. G., Lenggoro, I. W. and Okuyama, K., Polymer-assisted annealing of spray-pyrolyzed powder for formation of luminescent particles with submicron and nanometer sizes. *J. Am. Ceram. Soc.*, 2007, **90**, 425–432.